

Multivariate assessment of outflow water quality in highly urbanized creek system: implication of natural and anthropogenic processes

Umesh Kumar Pradhan*, Anirudh Ram Sukkhu Jaiswar, Balaram Sahu, Udayakrishnan Pallikkottathil Balakrishnan, Saurabh Lonkar, Laxmankumar Kumbhar

CSIR–National Institute of Oceanography, Regional Centre,
Lokhandwala Rd. Andheri (W), Mumbai, 400053, India

Abstract

Nutrient source and transport study in tropical creeks adjacent to megacities are sparse on a regional and global scale. High-frequency chemical data collected during 2017-18 in the Thane creek system, the largest micro-tidal urbanized creek in Asia, analysed to assess the chemical water quality, with its linkage to different hydrological stages (monsoon, post- and pre-monsoon) and ongoing anthropogenic activities. Cluster analysis indicates typical zonation between creek outflow and nearshore waters with distinctive physicochemical properties. The creek outflow upholds substantial amounts of nutrient and suspended sediment due to turbid-water movement from the ephemeral mudflats and anthropogenic dredging. The year-round hyper-turbid condition in the bottom water triggers the addition of disproportionate nutrients (9 % dissolved inorganic nitrogen (DIN) and 14 % reactive phosphorous (PO_4^{3-})) in the outflow region. The DIN and PO_4^{3-} removal up to 10 and 35 %, respectively, occurs in the nearshore region; sedimentation, which acts as a sinking interface for nitrogen and phosphorous, also causes shifting in their limiting conditions. The hyper-turbid condition causes removal of dissolved silicate (DSi) by 5 % in the entire region. Ammonium (NH_4^+), mainly sourced from the sewage in outflow waters efficiently mineralized. Chemical indexing of water highlights that the bottom water column remained un-supportive to the balanced ecology. The findings of this study have implications for other tropical creek-estuary concerning management strategies against inadequate flushing. The stalled nutrient export affected balance ecology in tropical Thane creek need attention to accurately understand the adjacent marine environmental impact and form effective mitigation policies.

Keywords: Turbidity; nutrient; water quality index; urbanization; Thane creek system

1. Introduction

The ecological bearing of tropical creek systems is sparsely studied globally; nevertheless, they support significant material transport compared to the estuaries with diverse hydrological characteristics. Creek systems with high surface-to-volume ratio and low-energy have collective importance in ecological processes, flood control, stormwater discharge, and biological habitat sustainability to wildlife. Unlike the upland draining creeks those governed with the freshwater flow, mesohaline creek systems often debouch into bay and harbours supportive to anthropogenically influenced complex food webs (Dame et al. 2000; Posey et al. 2002). Ecological imbalance owing to processes such as land use modification, dredging, sewage-nutrient load and overuse of biological resources have been markedly noticed in tropical creeks during the past decade (Lohrer and Wetz 2003; Emmanuel and Onyema 2007; Baliarsingh et al. 2013; Marmontel et al. 2018; Thanh-Nho N et al. 2020). Large-scale anthropogenic disturbances such as regular deepening activities potentially enhance the turbidity level following the release of bio-stimulatory nutrients and toxic metals and disturb the benthic habitat diversity pattern (Livingston 1996). Similarly, changing concentrations of suspended particulate matter and nutrients to several times higher than the concentration during natural precipitation collectively hamper water quality and ecosystem function (Mallin and Lewitus 2004; Quadros et al. 2009).

Enhanced sources of nutrients and contaminants influence creek systems in tropical peninsular India discharged through river-estuaries during seasonal precipitation and anthropogenic input, which affect their nutrient chemistry and biological functioning (Natesan et al. 2017; Sahu et al. 2013). Thane creek system (TCS), the largest in the Asian sub-continent, is overwhelmed against its assimilative capacity for sewage (Sasmal et al. 2007; Vijay et al., 2014, 2020); also, the inadequate tidal circulation scarcely favours efficient removal of the contaminant (Naidu and Sarma 2001; Gupta et al. 2004; Nayak and Balaji 2016). Previous studies in the mesohaline region of the creek have remarked with semi-permanent hypoxia, hyper-turbid waters, enriched nutrients (Quadros et al. 2001) and heavy metals (Zingde and Govindan 2000; Singare et al. 2010) those correspond to alteration in biota composition as well as substitution with high pollutant-tolerant species (Quadros et al. 2009). The outflow region of TCS accommodates the two largest ports of India (Jawaharlal Nehru Port (JNP) and Mumbai Port (MbP)) and virtually receive turbid waters through ephemeral creeks, mudflats, sewage outlets etc. The hyper-turbid waters from the mudflats and regular deepening activities that may affect nutrient chemistry and ecology remain sparsely studied. The prime objectives of this study are (i) to ascertain natural and anthropogenic processes associated with the nutrient composition across their transportation route from outflow to nearshore region and (ii) to highlight the forces on the nutrient

characteristics and chemical water quality significant to the ecological sustainability status of TCS. The observational approach through high-frequency sampling used first of its kind in the system broadly highlights the influence of seasonal hydrologic stages, high suspended load, inadequate hydrodynamic and periodic deepening on cycling and delivery of nutrients in TCS. Given that the developmental activities due to population rise would invariably increase in TCS within the next few decades, the present study will have direct relevance with management decisions in predicting the ecological balance of the creek.

2. Materials and Methods

2.1 Study area description

The TCS is a second-order tributary of the Ulhas river system, with its confluence in the mid-estuarine region (Figure 1). The creek debouches into the Arabian Sea through a funnel-shaped bay (width:100-9000 m; Vijay et al. 2020), which serves as a significant waterway for JNP and MbP activities. The creek's maximum water depth is 12 m at the sea interface, decreasing the upper regime. The creek has two major mudflats corresponds to the substantial delivery of finer sediment and numerous tidal inlets draining into the main channel, which horizontally divides the lower creek region into two parts (Sastry 1971). Semidiurnal spring tides (range: 4.5-5.0 m) are prevalent at the sea interface (Chouksey et al. 2004). The entrapment of tidal water within upper reaches during the flood-ebb cycle is significant ($10 \times 10^3 \text{ m}^3$; Swamy and Satyanarayan 1984). Generally, the TCS experience tropical hot-humid weather throughout, with an average precipitation of 2500 mmyr^{-1} majorly during southwest monsoon (SWM). Summer and winter temperature ranges are $35\text{-}40 \text{ }^\circ\text{C}$ and $25\text{-}35 \text{ }^\circ\text{C}$ (Environmental Status Report 2010). The entire catchment (1226 km^2) upholds one of the densest industrial setups (e.g., Mumbai) in the country. The population per unit area within the major municipalities' ranges between ~ 3000 to $37000 \text{ inhabitants km}^{-2}$, with an average of $11500 \text{ inhabitants km}^{-2}$ (Census Report 2011), which is two-order of magnitude higher than the country's population density. The creek water quality is primarily affected by the wastewater generated from the industries and domestic usage, which discharged along the creek. The daily discharge of wastewater through allocated outlets within the creek is increased nearly two-times from $\sim 6 \times 10^6$ to $11 \times 10^6 \text{ L day}^{-1}$ between 2001 and 2015 (Gupta et al. 2004).

2.2 Sampling and pre-treatment

Water samples were collected weekly on TCS between September 2017 and February 2019 at eight locations covering 35 km (in $\sim 200 \text{ km}^2$ area) across the outflow regions and adjacent coastal waters (up to $\sim 10 \text{ km}$ from the shoreline). The sampling points are located within the close proximity

of channel and represents the maximum flow in the creek. The samples collected were from the surface and bottom water column during neap tide periods (tidal height 1 to 1.5 m) using a 5L Niskin water sampler (General Oceanic USA). Hydrographic parameters [temperature, pH, salinity, suspended particulate matter (SPM) and turbidity] were measured in weekly collected samples, whereas inorganic nutrients [nitrite (NO_2^-), nitrate (NO_3^-), ammonium (NH_4^+), phosphate (PO_4^{3-}) and silicate (DSi)] were measured fortnightly. Sample collection during July and August was stopped due to operational difficulties.

Meteorological data such as average monthly rainfall during 2017-19 and their long-term limits (1982-2012) of station-derived precipitation records were collected from the Indian Meteorological Department at seven locations covering upper and lower TCS (Figure 1).

2.3 Hydrography and nutrient measurement

Water temperature (T) and pH were measured in situ using a CTD (Model: Plus, X CTD; AML Oceanographic) and multi-parameter probe (Model: Orion Star A111; Thermo Scientific Ltd.), with analytical precisions 0.01°C and 0.005 pH unit, respectively. Water samples for nutrient analyses were collected in acid-cleaned polythene bottles, stored in cool conditions ($\sim 4^\circ\text{C}$) immediately after collection and analysed within 5 hours of collection at the shore laboratory CSIR-National Institute of Oceanography, Mumbai. Water samples were filtered through pre-cleaned-weighed cellulose acetate filters (pore size: $0.45\ \mu\text{m}$; Millipore). The filters were oven-dried at $50\text{-}55^\circ\text{C}$ till constant weight and weighed again. The difference in weight was used to determine suspended particulate matter (SPM) concentration. Salinity was determined using an “Autosal” Laboratory Salinometer (Model: Guideline 8400B; Guideline Instruments Ltd.) based on continuous flow through a conductivity cell at a selectable temperature range technique. International Association for the Physical Sciences of the Oceans (IAPSO) standard seawater (salinity: 34.995; Ocean Scientific International Ltd.) was used to calibrate the instrument. Chloride concentrations were calculated from the salinity-conductivity relationship (Cox et al. 1967). Turbidity was measured in a Nephelometer based on the percent transmittance method (Model: Orion AQ4500; Thermo Scientific Ltd.). The US-EPA-approved SDVB primary turbidity standards (0.02-1000 NTU) were used for instrument calibration. Analytical precision for salinity and turbidity were 0.001 PSU and $\leq 5\%$, respectively as obtained by repetitive measurement of a same sample during this study.

Concentrations of inorganic nutrients and dissolved oxygen (DO) were analysed as per methods described by Grasshoff et al., (1983). Briefly, samples for DO were fixed onboard by adding Winkler’s reagents A (Manganous Chloride; MnCl_2) and Winkler’s B (alkaline Sodium Hydroxide-potassium

iodide; NaOH/KI). The precipitate so formed was decomposed with 50% Hydrochloric Acid (HCl) and the released iodine (I_2) was titrated against standardized sodium thiosulphate ($Na_2S_2O_3$) using a digital titration system (Model: Dosimat Plus 876; Metrohm AG). To determine biochemical oxygen demand (BOD), the DO was determined after incubation of samples for 3 days at 27°C. The difference in DO concentrations on the first and third day yielded biochemical oxygen demand (BOD; Grasshoff et al. 1983). Inorganic nutrients (NO_2^- , NO_3^- , NH_4^+ , PO_4^{3-} and DSi) in all the samples were analysed in duplicates by colorimetric method using a SKALAR segmented flow auto analyser. Seawater nutrient standards (OSIL, UK) and in-house standards were used to check nutrient measurement reproducibility. Analytical precision was checked by repetitive measurements for NO_2^- , NO_3^- , NH_4^+ , PO_4^{3-} and DSi, obtained at 0.01, 0.07, 0.1, 0.02 and 0.2 μM , respectively. The dissolved inorganic nitrogen (DIN) concentration is expressed as sum of NO_2^- , NO_3^- and NH_4^+ . The concentration of sulphate (SO_4^{2-}) was determined gravimetrically using Barium Chloride ($BaCl_2$) precipitation technique (Grasshoff et al. 1983), with an analytical precision of $\leq 5\%$.

2.4 Statistical analysis and assessment index

Altogether nearly 800 data points were segregated monthly and seasonally and their statistical variance was checked at significant confidence intervals $p \leq 0.05$ (95%) and $p \leq 0.01$ (99%) using one-way analysis of variance (ANOVA), after the Komogorov-Smirnov normality test. Normalization of data using the Z-scale transformation method was preferred to minimize the mis-classification in data dimensionality. Parameters such as salinity, T , DO and BOD representative for hydrography were used in cluster analysis to identify the classification among sampling regimes. The Ward's method (linkage between groups and Euclidian distance measure) was preferred and suitable for aquatic environment studies (Shirodkar et al. 2009). Similarity within the groups was identified through seasonal data displayed in dendrograms that were influenced by similar chemo-dynamic properties during different seasons. Inter-relationship among the parameters was checked through Pearson's correlation analysis. Principle Component Analysis (PCA), with rotated component matrix analysis, was performed to understand forcing on nutrient chemistry. Parameters such as T , pH, salinity, DO and BOD are considered indicators of hydrography condition, concentrations of NO_2^- , NO_3^- , NH_4^+ , PO_4^{3-} and DSi as nutrient, with Cl^- and SO_4^{2-} as supplementary for marine characteristics. Statistical package for the social sciences (SPSS.16; USA Inc.) was used to perform cluster analysis, PCA, ANOVA and Pearson's correlation.

In this study, a chemical water quality index (C_{WQI}) using multivariate data is proposed, which helped alleviate the information on ecological-sustainability status around creek outflow and nearshore region. The C_{WQI} is based on the arithmetic average technique described in Brown et al.

1970, later modified and used in various studies (Prati et al. 1971; Gupta et al. 2003; Kachroud et al. 2019). The CWQI is a vital proxy used to classify water quality in the coastal region, therefore helping keep policymakers and the general public aware of the ecological health status of the water body. The arithmetic average approach used in this study is one of the popular methods (Gupta et al. 2003), primarily focused on weighing of multivariate parameters in the coastal water. The standard limits for hydrography, nutrient and marine components were adopted from their prescribed and observed values around Indian continental margin and the tropical coastal region. The standard limits (mean and standard deviation) and the uncertainties within the seasonal cycle and anthropogenic activities were simulated using the Marcov chain Monte Carlo method to deal with the standard limit variability straightforwardly. The C_{WQI} was calculated using the standard limit of multivariate parameters as follows;

$$C_{WQI} = \sum_{i=1}^n \left(\frac{W_i \times Q_i}{W_i} \right) \quad (1)$$

Where W_i and Q_i are calculated as below;

$$W_i = k \times \sum_{i=1}^n \left(\frac{1}{S_i} \right) \quad (2)$$

$$k = \frac{1}{\sum_{i=1}^n \left(\frac{1}{S_i} \right)} \quad (3)$$

$$Q_i = \left(\frac{Q_s - Q_p}{S_i - Q_p} \right) \times 100 \quad (4)$$

In above equations, W_i and Q_i are the calculated unit weights and quality ratings of the multivariate parameters, respectively. Proportionality constant ' k ' is calculated using the standard limit i.e. ' S_i ' of the parameter, which is adopted from literature across Indian continental margin provided in the foot note of Table 1. Measured sample limit is expressed as Q_s . The permissible limits (Q_p) are the limits described for the coastal water classes II, III and V mainly used for industrial and fishery activities (Central Pollution Control Board 2006). The marine water quality based on

hydrography and nutrient properties primarily responsible for sustainable and healthy ecosystem were scored on a scale from 0-25 (Very bad), 26-50 (Bad), 51-70 (Moderate), 71-90 (Good) and 91-100 (Very good).

3 Results

The majority of the rainfall occurred during the SWM (June-September) during 2017-18. Location-derived monthly precipitation data indicated SWM rainfall equals 95% of total annual rainfall in TCS (Figure 2a). Proportionally, mean monthly rainfall during 2017-18 was similar with long-term (1982-2012); however, the catchment averaged data demonstrated significant variation of precipitation between upper and lower reaches (Figure 2b). Besides, roughly ten-times higher rainfall in upper TCS during November 2017 and nearly eight-times higher rainfall in lower TCS during December 2017 correspond to low-level trough and cyclone (Ockhi), respectively. The entire studied region constitutes two significant segments in cluster analysis, namely, nearshore (stations 1-4) and outflow (stations 5-8) regions, which implies geographic restraint of hydrographic properties (Figure 3). The exception to this pattern during SWM, attribute to the protraction of outflow waters.

3.1 Hydrographic characteristics

Seasonally averaged hydrography, inorganic nutrient and stoichiometries in surface and bottom layers of clustered segments are presented in Tables 1 and 2 and their monthly variation in Figure 4-6. The distribution of T in both segments exhibited parabolic trends similar to the air temperature (Figure 4). The surface and bottom T follow closely without any significant stratification in outflow and nearshore during all seasons (Table 1). Seasonally, T in surface (SWM: 28.7 ± 1.1 °C; post-monsoon: 28.4 ± 1.4 °C and pre-monsoon: 27.9 ± 1.6 °C) and bottom (SWM: 27.9 ± 0.9 °C; post-monsoon: 27.8 ± 1.8 °C and pre-monsoon: 27.7 ± 1.6 °C) changed significantly ($p < 0.01$ and < 0.05 , respectively; Table 1). pH was alkaline (> 7) in both segments irrespective of seasonal hydrological changes and higher pH was in nearshore than the outflow segment, without any variation between surface and bottom (Figure 4). Between surface and bottom, salinity changed significantly in both the segments (Table 1). Seasonally, salinity levels in surface (SWM: 30 ± 5.1 PSU; post-monsoon: 34 ± 1.4 PSU and pre-monsoon: 35 ± 0.9 PSU; $p \leq 0.01$) and bottom (SWM: 33.5 ± 2 PSU; post-monsoon: 34.3 ± 1.2 PSU and pre-monsoon: 35 ± 0.8 PSU) changed significantly and in outflow, the salinity was higher in pre-monsoon and lowered during SWM (Figure 4). SPM in bottom (SWM: 872 ± 1418 mg/L; post-monsoon: 836 ± 1294 mg/L and pre-monsoon: 574 ± 601 mg/L) were nine-fifteen times higher than that in surface (SWM: 78 ± 84 mg/L ; post-monsoon: 58 ± 56 mg/L and pre-monsoon: 65 ± 54 mg/L), shows seasonal significance in both segment ($p \leq 0.01$; ANOVA; Table 1). During the entire

study, SPM varied between 8 and 5562 mg/L, with significantly higher values in the outflow waters ($p < 0.01$; ANOVA; Table 1; Figure 4). Mean monthly turbidity of surface and bottom water in both segments closely match SPM (Figure 4). Mean monthly DO was relatively low in the outflow than in the nearshore. DO in surface (SWM: 5.8 ± 0.7 mg/L; post-monsoon: 5.3 ± 1.2 mg/L and pre-monsoon: 5.7 ± 0.7 mg/L) was significantly higher than bottom (SWM: 3.1 ± 1.7 mg/L; post-monsoon: 3.9 ± 1.3 mg/L and pre-monsoon: 4.9 ± 0.8 mg/L) in both the segment (Figure 4). Surface and bottom DO levels of both the segments decreased during late SWM and post-monsoon (outflow: 2.4 mg/L; nearshore: ≤ 1 mg/L). The surface and bottom BOD changed significantly during different seasons in both the segments (Table 1). Extremely higher bottom BOD was during September (outflow: 4.5 mg/L; nearshore: 11 mg/L), which coincided with lowered DO (Figure 4).

3.2 Concentration and molar ratios of nutrients

The water column nutrients highlighted higher loads of NO_3^- and DSi relative to PO_4^{3-} and NH_4^+ , with significant variation in stoichiometric ratios across the outflow-nearshore gradient (Table 1; Figures 5 & 6). On average, PO_4^{3-} , NO_3^- and DSi in surface display significant seasonal differences in both segments (Table 2). NO_2^- contribution to DIN ($\text{NO}_3^- + \text{NO}_2^- + \text{NH}_4^+$) is low in SWM (6 %) and high in pre-monsoon (13 %). Whereas the contribution of NH_4^+ to DIN is comparable during SWM (13 %) and pre-monsoon (14 %), with minimal changes in NO_2^- and NH_4^+ during post-monsoon. Outflow waters (surface and bottom) exhibit 2-3 times higher PO_4^{3-} than nearshore. On average, mean PO_4^{3-} in surface (SWM: 3 ± 1.6 $\mu\text{mol/L}$; post-monsoon: 1.9 ± 0.8 $\mu\text{mol/L}$ and pre-monsoon: 2.8 ± 1.7 $\mu\text{mol/L}$) was lower than bottom (SWM: 3.5 ± 4.8 $\mu\text{mol/L}$; post-monsoon: 2.7 ± 1.3 $\mu\text{mol/L}$ and pre-monsoon: 3.5 ± 1.8 $\mu\text{mol/L}$), without any seasonal significance ($p > 0.05$; Table 1). The PO_4^{3-} levels in the outflow and nearshore segment vary positively with SPM (Table 3). Water column NO_3^- was three times higher in outflow than the nearshore, without much difference in surface and bottom (Table 2). However, the NO_3^- in surface (SWM: 21.6 ± 14.1 $\mu\text{mol/L}$; post-monsoon: 13.3 ± 12.3 $\mu\text{mol/L}$ and pre-monsoon: 14 ± 8.8 $\mu\text{mol/L}$) and bottom (SWM: 22.2 ± 16.6 $\mu\text{mol/L}$; post-monsoon: 13.2 ± 8.8 $\mu\text{mol/L}$ and pre-monsoon: 13.7 ± 9 $\mu\text{mol/L}$) was higher during SWM and display seasonal variation ($p < 0.01$; Table 2, Figure 5). Surface and bottom NH_4^+ levels were more or less similar in outflow and nearshore, except that in September, six-times higher surface NH_4^+ noticed in outflow than the nearshore (Figure 5). NH_4^+ values were scattered, without showing any statistical significance among the seasons, segments, and surface vs. bottom (Table 2). No significant correlation was found between nitrogen species and DO in the outflow waters, except the nearshore waters display negative correlation of DO and NO_2^- during SWM and post-monsoon. The water column DSi in outflow waters was two times higher than that in nearshore. Mean monthly DSi was nearly similar at outflow and

nearshore during May and June (Figure 5). Seasonally, average DSi in surface (SWM: 48.9 ± 18.7 $\mu\text{mol/L}$; post-monsoon: 32.1 ± 13.4 $\mu\text{mol/L}$ and pre-monsoon: 22.9 ± 9.6 $\mu\text{mol/L}$) was more or less similar with the bottom (SWM: 41.7 ± 12.4 $\mu\text{mol/L}$; post-monsoon: 36.4 ± 12.3 $\mu\text{mol/L}$ and pre-monsoon: 29.5 ± 11.4 $\mu\text{mol/L}$) (Table 2).

Molar nutrient ratios *viz.* NO_3^- : PO_4^{3-} vs. Dsi: PO_4^{3-} , showed distinct variations in surface and bottom of outflow and nearshore segments (Figure 6). The surface and bottom NO_3^- : PO_4^{3-} were lower than the Redfield ratio of 16:1 (Redfield et al. 1963) in outflow and nearshore during all the seasons highlighted depletion of NO_3^- relative to PO_4^{3-} (Figure 6). Overall, mean NO_3^- : PO_4^{3-} in surface (SWM: 6.8 ± 2.7 ; post-monsoon: 7.8 ± 4.5 and pre-monsoon: 9.1 ± 19.6) was more or less similar with the same in bottom (SWM: 7.3 ± 4.6 ; post-monsoon: 10.4 ± 45.7 and pre-monsoon: 6.8 ± 9.7). The surface and bottom NO_3^- : PO_4^{3-} values of nearshore segment were higher during pre-monsoon (Figure 6). Significant variation in surface and bottom NO_3^- : PO_4^{3-} was noticed across outflow-nearshore gradient during SWM ($p < 0.01$; Table 2). Mean NO_3^- : DSi ratio within the surface and bottom waters of nearshore and outflow segment were lower than the value of 1:1, considered for balanced growth of diatoms (Brzezinski 1985). The seasonal mean of NO_3^- : DSi within the surface and bottom waters of outflow, as well as the nearshore segment, were < 1 , indicative towards DSi rich relative to NO_3^- in the region. However, during pre-monsoon NO_3^- : DSi in surface and bottom of outflow segment showed higher (> 1) ratios (Figure 6). Overall, change in NO_3^- : DSi across outflow-nearshore gradient was significant in the surface and bottom during SWM and pre-monsoon ($p < 0.01$; Table 1). Seasonally, mean DSi: PO_4^{3-} in surface (SWM: 19.1 ± 7.3 ; post-monsoon: 16.3 ± 11.7 and pre-monsoon: 15.1 ± 24.8) and bottom (SWM: 17.4 ± 10.8 ; post-monsoon: 18.3 ± 52.8 and pre-monsoon: 12.4 ± 15.3) were close to 15:1, presumed to be suitable for composed growth of diatoms. Seasonal changes in DSi: PO_4^{3-} at outflow vs. nearshore were not significant. Concentrations of SO_4^{2-} were more or less similar, varied between 2.2 g/kg and 2.6 g/kg in surface and bottom waters of outflow as well as nearshore region during this study (Table 2). The SO_4^{2-} : Cl^- ratio linearly mixed at the high salinity and varied between 0.11 ± 0.03 and 0.14 ± 0.01 , close to seawater (Morries and Riley 1966). SO_4^{2-} : Cl^- represented mostly non-conservative relationship (salinity vs. SO_4^{2-} ; Pearson's $r = 0.6-0.9$; Table 3) during SWM and pre-monsoon seasons at outflow as well as nearshore segment. SO_4^{2-} : Cl^- deviated from the seawater slope (0.14) within the outflow segment during post-monsoon due to lower surface SO_4^{2-} value.

3.3 Factors influencing water quality

Principal components influencing the water quality were derived from area-averaged seasonal data within both segments. PCA results highlighted two prime factors described more than 75% of

data variances, affecting the nutrient chemistry within outflow and nearshore (Figure 7). In the outflow, Factor 1 was associated with strong positive loadings of T , NH_4^+ and DSi , along with the weak association of NO_2^- , NO_3^- and BOD, with a fairly positive correlation among them. Factor 2 was associated with strong positive loadings of SPM and turbidity along with PO_4^{3-} and negative loadings of NO_2^- and DO. In nearshore, the Factor 1 was associated with positive loadings of SO_4^{2-} , Cl^- , NH_4^+ and NO_2^- , with negative loadings of PO_4^{3-} , NO_3^- and DSi . Similarly, Factor 2 was associated with strong positive loadings of BOD, SPM and turbidity, and negative loading DO. The majority of the nutrients (PO_4^{3-} , NO_3^- and DSi) in both segments were associated with SPM highlighting turbid-water influence. In both the segments, DO appears in the left quadrant negatively related to SPM during post and pre-monsoon seasons. The chemical quality of water evaluated through arithmetic average against the standard limits indicated moderate to good water quality ($C_{\text{WQI}} > 60-90$) in the outflow and nearshore segment. However, based on the stoichiometric ratios, sporadic deviations highlighted the unsupportive bottom water condition towards biological sustainability in TCS in both segments (Figure 7).

4. Discussion

On a unit area basis, ~90% of the annual seaward nutrient export through monsoonal Indian estuaries occur during SWM, and the persisted 10% transferred through sluggish water discharge during non-monsoon are mostly anthropogenically derived (Pradhan et al. 2014). Seasonal variability of hydrographic and nutrient parameters in TCS bear a resemblance to minor timescale change, majorly linked with meteorological factors and hydro-physical properties of water masses that varied in a longitudinal gradient and controlled the creek water quality (Figure 2). The statistical analyses (cluster) revealed precise segmentation of the area relative to geographical domination of hydro-physical properties (Figure 3). The outflow waters appeared to be holding essential nutrients, disseminated from anthropogenic activity surged upper region during SWM and uneven rainfall during post-monsoon. Nearshore region witnessed coastal characteristics along with an extended creek outflow during SWM. Seasonal monsoon winds considerably influenced T all along the lowlands of Western Ghats in SWM and hot-humid weather in post- and pre-monsoon (Reddy and Rao 1994). Impact of low-salinity water influx from the upper reaches corresponds to lower salinity of outflow waters in SWM. Over a large window of pre-and post-monsoon, alkaline conditions prevailed in outflow region due to seawater exchanged through small creeks and nearshore waters. Relatively lower pH of outflow waters can be related to lowered semi-diurnal tidal amplitude, with minimum phase delay during pre-and post-monsoon, which upholds sluggish water flow during neap tide (Thomas et al. 2019). Due to inadequate freshwater runoff, salinity fluctuation across the outflow-nearshore

gradient was minimal in TCS. However, the outflow waters exhibited lower salinity during September influenced by the excessive rainfall in the lower TCS.

4.1 Oxygen susceptibility in turbid Thane creek system

The micro-tidal condition in TCS favours inadequate flushing, water mass mixing and defensive stratification owing to tapered-shallow (width: ≤ 100 m; depth: ≤ 4 m) water column in the upper mesohaline region. In the outflow region (width: ~ 6 km; depth: 8-10 m), bifurcation of water masses causes a high residual current that triggers intense mixing and gives rise to year around semi-permanent turbid condition (Naidu and Sarma 2001; Gupta et al. 2004). The non-conservative mixing of turbid waters across outflow-nearshore gradient is related with sluggish flushing and greater SPM retention capacity. The SPM retention calculated using their seasonal mean values within the surface and bottom layers of the outflow segment were 50-65 % and 60-75 % (Adam et al. 2010).

The impact due to the low-temperature turbid water supplied by the minor creeks and mudflats into outflow (SPM vs. T : $r = -0.66$ (surface); -0.77 (bottom) ; $p < 0.01$) and nearshore (SPM vs. T : $r = -0.89$ (surface) ; $p < 0.01$) region is significant, also affected by the SWM precipitation and uneven extreme meteorological condition during post-monsoon. The low-temperature turbid waters associated with high surface salinity in outflow (SPM vs. salinity: $r = 0.54$ (SWM); $r = 0.49$ (post-monsoon) ; $p < 0.01$) highlight towards meagre impact of freshwater associated SPM. Provided that the mesohaline region of TCS is extremely turbid (SPM = 1.5×10^3 - 11.5×10^3 mg/L; Quadros et al. 2004), the outflow region is not a perfect fluvial SPM trap due meagre flushing and dominance of mudflat, also anthropogenic activities such as periodic deepening of the channel. The SPM values of outflow segment bears resemblance with the SPM values generally observed in the estuaries affected by seasonal turbidity maxima along peninsular India (Rao et al. 2011). Moreover, the surface SPM in outflow were close to the limits of SPM found in large tropical turbid estuaries elsewhere (Pearl estuary, PRC: 103 mg/L; Li et al. 2017). The year around high bottom SPM accentuates the permanent turbidity maximum zone (TMZ), which outspread between the outflow and nearshore region of TCS, similar to hyper-turbid estuaries elsewhere (Ems, UK: SPM 15×10^3 mg/L; Winterwerp et al. 2017). Salinity is erratically related with SPM in the bottom layers of the outflow segment, highlighting wind instigated stratification that limits the vertical migration of bottom TMZ. Relative association between SPM and salinity occurs, mostly in surface layers of outflow and nearshore during SWM and post-monsoon can be due to intervals during re-suspension (deNijsetal et al. 2010). Such condition nonetheless restricts the longitudinal movement of bottom TMZ, causing outflow to become independent of high turbid surface water supply to the nearshore. The impact of wind on surface turbidity at outflow cannot be

ruled out as the surface SPM were higher throughout (>50 mg/L; Table 1; Kessarkar et al. 2009). Wind speed (4 m/s) that can affect surface current velocity is significant in TCS (Gupta et al. 2004).

Generally, the surface and length that primarily govern the flushing efficacy relative to fluvial discharge in creek-estuary systems can subside DO levels during prolonged residence time (Schmidt et al. 2019). The presence of permanent post- and pre-monsoon hypoxia in the upper mesohaline region (DO: ~ 2 -2.7 mg/L), improves during SWM (DO: 3.5-4.5 mg/L), is largely controlled by the localization of anthropogenic activities, such as urban runoff, sewage discharge etc. (Quadros et al. 2004). However, this does not turn up to be primarily impelling into the outflow and nearshore regions, distinguished higher water column DO (>3 -6.5 mg/L; DO_{sat} : 70-100 %; Table 1; Figure 2), sustainable for biodiversity. Inadequate water exchange between outflow and the upper regime is the key reason for the entrapment of a significant fraction of hypoxic turbid waters in the swampy mangrove system, which partially gets delivered to outflow region during the spate events. Lower DO levels in outflow compared to nearshore related with multiple processes, e.g., light inhibition due to turbid waters that hinder photosynthesis and atmospheric gas exchange (Lanoux et al. 2013), heterotrophic degradation of organic matter and disparity in oxygen saturation due to high SPM at given T and salinity. The latter two processes were predominated in TCS as indicated by weak correlations of DO vs. SPM during different seasons. On a seasonal scale, T is the prime controlling factor for DO variability, indicative through DO vs. T in outflow (surface: post-monsoon $r = -0.40$; $p < 0.05$; bottom: post-monsoon $r = -0.43$; pre-monsoon $r = -0.30$; $p < 0.05$ and < 0.01 , respectively; Table 3) and in nearshore (surface: pre-monsoon $r = -0.34$; $p < 0.05$; bottom: post-monsoon $r = -0.31$; pre-monsoon $r = -0.45$; $p < 0.05$ and < 0.01 , respectively), non-existence in SWM. Salinity appeared to be the second controlling factor, negatively correlated with DO in surface and bottom layers of nearshore during SMW. Salinity vs. DO was positively correlated in surface and bottom layers of entire region during pre-monsoon season, with scattered relationships during post-monsoon (Table 3). The bottom layers of outflow and nearshore remained hypoxic during late SWM associated with higher BOD, SPM and salinity, presumably indicative of DO consumption due to organic matter oxidation, which, however, recovers during post- and pre-monsoon seasons. The bottom TMZ in TCS may likely to prevent primary production during most times of the year; also, the SPM mainly enhanced through bed re-suspension increased the organic content due to sewage (Sasmal et al. 2007; Vijay et al. 2010; 2020). Overall, the creek outflow region persisted with oxygen susceptible condition due to low-temperature high-salinity characteristics in bottom water during post- and pre-monsoon, also within surface and bottom layers of nearshore during pre-monsoon.

4.2 Seasonal nutrient chemistry in lower Thane creek

Lateral mixing of exported nutrients and phytoplankton utilization are primary drivers of surface nutrient chemistry, whereas biological respiration and bacterial remineralization of sewage and particulate organic matter correspond to the bottom nutrient composition in TCS (Zingde and Govindan 2000; Quadros et al. 2001; Sasmal et al. 2007). Enriched NO_3^- and NO_2^- in outflow was due to the balance between disproportionate addition and poor flushing (Figure 5). The outflow NO_3^- and NO_2^- maxima during SWM were similar to other monsoonal systems in India (Pradhan et al. 2014). Significant amounts of NO_3^- (~45 %) and PO_4^{3-} (~35 %) received during SWM from the upper mesohaline region, which remains norm-oxic and NO_3^- deficit during peak freshwater runoff condition, thereby turned hypoxic and nutrient-rich (5-6 times higher), with the hyper-turbid condition during the post-and pre-monsoon (Quadros et al. 2004). The turbid water-associated nutrients delivery through ephemeral creeks, mudflats, and anthropogenic deepening activities hampers the efficient exchange between upper and outflow waters. Mean monthly NO_3^- varied inversely with NO_2^- in surface and bottom layers of outflow and associated with invariable NH_4^+ , together indicated nitrification i.e., production of NO_3^- from NO_2^- (Figure 5). Alternatively, increased NO_2^- and NO_3^- , with invariable NH_4^+ during pre-monsoon, demonstrated the inhibition of NO_2^- oxidation and was negatively influenced by SPM, similar to large tropical estuaries (Dai et al. 2008). Water column NH_4^+ was exceptionally higher during late SWM (September) in the outflow and associated with relatively lowered DO, SPM and NO_3^- , with a higher NO_2^- indicating inhibition of NO_2^- oxidation (Figure 4 & 5). Alternatively, nearshore waters with increased NO_3^- and decreased NO_2^- , with insignificant variable NH_4^+ during post-monsoon indicated nitrification.

The negative relationship of salinity with NH_4^+ during SWM, with NO_2^- during post-monsoon and with NO_2^- and NO_3^- during pre-monsoon, altogether related negatively with SPM in outflow (post-and pre-monsoon) indicative towards nutrient utilization in biological processes. The nearshore surface water mainly receives turbid water-associated nutrients (NO_3^- and NH_4^+) during SWM and post-monsoon, indicated through positive variation of SPM with NO_3^- and NH_4^+ . During most sampling months, a weak inflow of freshwater was evident, which also explained the limited freshwater source of nutrients into the outflow. Therefore, a large proportion of NH_4^+ mainly sourced from sewage within the lower reaches and derived from mesohaline regime gets efficiently mineralized and contributes to nitrogen cycling, with the minimal recognizable trend of NH_4^+ (Bruesewitz et al. 2015). PO_4^{3-} concentrations were higher in outflow relative to nearshore, owing to the accumulation of PO_4^{3-} through human sewage and industrial wastes (Quadros et al. 2009). The difference in annual values highlighted ~35 % PO_4^{3-} drawdown into the bottom layer of nearshore waters, whereas ~15 % removal

of PO_4^{3-} from bottom layers of outflow, probably due to re-suspension. The PO_4^{3-} remained positively associated with SPM throughout and significantly correlated in bottom water of nearshore (post-monsoon) and surface water of outflow (pre-monsoon). The DSi variation across the year was not significant, and ~5 % of DSi removed in both the segments due to loss as biogenic form or lateral transportation. The conservative mixing DSi across the outflow-nearshore gradient is prominently noticed through salinity vs. DSi (negative) relationship during SWM and in outflow, during post-monsoon due to excess rainfall. However, bottom re-suspension accompanied with higher SPM gives rise to higher DSi in the outflow during pre-monsoon, enhancing mineral silica present in the sediment. The utilization of DSi by the phytoplankton under low-turbid condition in outflow segment cannot be ruled out. Dissolved nitrogen species can be limited in the estuarine environment relative to phosphorous owing to excess sediment transport (Nixon 1995; Paerl 2009) and reduced sedimentation (Paudel et al. 2019). The outflow accumulates 9 % DIN and 14 % PO_4^{3-} through turbid bottom water, whereas the adjacent nearshore water drawdown almost 10 % DIN and 35 % PO_4^{3-} , which together indicated significant sinking of nitrogen and phosphorous within nearshore region. The conceptual model for additional an removal of nutrients are presented in supplementary Figure. PO_4^{3-} and NO_3^- are efficiently utilized by the phytoplankton in nearshore waters, amongst PO_4^{3-} values decline owing to consumption by the diazotrophs. However, the shift in preferential uptake of organic forms of nitrogen relative to inorganic could be potential reason for lower surface PO_4^{3-} and higher NO_3^- in nearshore waters (Kumar et al. 2017).

Variation in the stoichiometric nutrient pool was not significant across the seasons; however, the ratios displayed significant spatial variation in the investigated segments (Table 3). The cyclical pattern of monthly averaged inorganic nutrient stoichiometry within the surface as well as the bottom of outflow and nearshore segments, displayed lower $\text{NO}_3^- : \text{PO}_4^{3-}$ values (<16:1; Redfield) than the threshold limit over a significant window of the investigated period, which suggest high NO_3^- uptake as relative to PO_4^{3-} and faster recycling of PO_4^{3-} in outflow segment (e.g., Bhavya et al. 2016). The recycled PO_4^{3-} into the surface by bottom TMZ lowered the $\text{NO}_3^- : \text{PO}_4^{3-}$ ratio that displayed increased surface trend from pre to post-monsoon (Figure 6). PCA results indicated the association of nutrient with temperature and transitional shifts in $\text{NO}_3^- : \text{PO}_4^{3-}$ together highlight temperature as a prime factor for controlling outflow biological processes (Figure 7). Temperature-induced shifts in the limiting N:P ratio generally provoke nitrogen dependency of phytoplankton and bring on nitrogen limitation (Thrane et al. 2017). However, addition/removal of PO_4^{3-} and DSi exceptionally controlled the efficient recycling of TMZ nutrients, thereby instigating excess NO_3^- in the outflow during most seasons. Generally, NO_3^- limiting condition arises when $\text{NO}_3^- : \text{PO}_4^{3-}$ remain <16 and $\text{NO}_3^- : \text{DSi}$ is <1.

Similarly, both $\text{NO}_3^- : \text{PO}_4^{3-}$ and $\text{DSi} : \text{PO}_4^{3-} > 16$ can cause PO_4^{3-} limitation. Alternatively, $\text{NO}_3^- : \text{DSi}$ is > 1 along with $\text{DSi} : \text{PO}_4^{3-} < 16$, which will lead to DSi limitation in nearshore-coastal waters. The $\text{NO}_3^- : \text{PO}_4^{3-}$ values do not reveal unambiguously towards the transitional limitation of nitrogen (at lower $\text{NO}_3^- : \text{PO}_4^{3-}$) and phosphorous (at higher $\text{NO}_3^- : \text{PO}_4^{3-}$) in nearshore-coastal environment (Ptacnik et al. 2010). Therefore, a range of $\text{NO}_3^- : \text{PO}_4^{3-}$ around 16, will better explain the limitation of NO_3^- and PO_4^{3-} .

Both nearshore and outflow segments indicated higher $\text{DSi} : \text{PO}_4^{3-}$ (> 16 in $\sim 60\%$ of sample) during SWM and associated with lower $\text{NO}_3^- : \text{PO}_4^{3-}$ (< 16) and lower $\text{NO}_3^- : \text{DSi}$ (< 1), therefore indicative towards NO_3^- and PO_4^{3-} limiting condition. A significant portion (50%) of the data also showed lower surface $\text{DSi} : \text{PO}_4^{3-}$ in the outflow, with their $\text{NO}_3^- : \text{PO}_4^{3-}$ ranges canonical around 16:1 supportive more towards the recycling of PO_4^{3-} in surface by bottom TMZ (Figure 6). Therefore, disproportional variation in PO_4^{3-} holds substantial control of nutrient stoichiometry is also the reason for weaker seasonality of ratios in the outflow segment. Significant portion ($\sim 40\%$ of the data) within surface and bottom of outflow segment showed higher $\text{NO}_3^- : \text{DSi}$ (> 1) associated with low $\text{DSi} : \text{PO}_4^{3-}$ as well as $\text{NO}_3^- : \text{PO}_4^{3-}$ during pre-monsoon indicative of DSi limitation in the outflow region potentially due to higher biological abundance (diatoms; Painter et al. 2017). The nearshore waters remained PO_4^{3-} limited during pre-monsoon due to the bottom drawdown of PO_4^{3-} , which enhances $\text{DSi} : \text{PO}_4^{3-}$, under preferential utilization of NO_3^- (and DIN). In the nearshore waters, removal of PO_4^{3-} to the bottom caused dominance of transitional nitrogen species such as NH_4^+ and NO_2^- in the surface during late SWM. The same corresponds to why DO appeared in the left quadrant negatively affecting NH_4^+ and NO_2^- in PCA. Overall, the variability in stoichiometry of inorganic nutrient, which appeared to be changing seasonally as well as spatially in this study, highlighted that extrapolation of information using fixed nutrient molar ratio will not be unambiguous but certainly to be considered while assessing the trophic status and/or sustainability of the water towards biology.

4.3 Assessment of water quality and sustainability

Chemo-metrically evaluated water quality within outflow, and nearshore regions of TCS indicates good to a moderately altered condition. The use of stoichiometric ratios provided new insight highlighting favourability of nutrient chemistry towards biological sustainability in TCS (Figure 7). The C_{WQI} demonstrated longitudinal transformation across outflow-nearshore gradient and surface-bottom column. Nutrient ratios within the bottom of the outflow segment mostly remain unsupportive of the balanced biology, mainly relative to the enhanced turbidity and associated nutrient input from the ephemeral mudflow, periodic dredging, and sewage discharge, etc. The bottom layer of nearshore remains unfavourable for biological activity during late SWM. Surface layer indicated supportive

condition towards biological sustainability during early pre-monsoon, late SWM and early post-monsoon in both segments (Figure 7).

Catchment control and human interventions are the prime cause for excessive nutrient load in tropical creeks and estuaries. The nutrients such as DSi strongly related with runoff-temperature characteristics, whereas PO_4^{3-} is controlled by the weathering/erosion and anthropogenic fertilizer application (Maya et al. 2007; Liu et al. 2011). The present study on Asia's largest creek highlighted the significance of active in-system processes such as hydrodynamic condition and anthropogenic activities that cause enhanced turbid condition, affect nutrient limitation and seasonality, which is comparable with other turbid creek-estuary systems of the world. The PO_4^{3-} limiting condition resembled more with PO_4^{3-} recycling from turbid plume in outflow region affecting nearshore were previously noticed in other tropical regions such as Xiamen, the Chesapeake Bay, Gulf of Mexico, etc. (Harrison et al. 1990; Lohrenz et al. 1999; Sylvan et al. 2003; Kemp et al. 2005;). Given the condition that TCS would insatiably develop due to activities such as; expansion and deepening of ports, installations of more sewage outlets owing to the burgeoning population and shrinking of the vegetated lands into mudflats. Therefore, a real-time water quality indicating systems would be a potential need to understand this largest creek's balanced ecological condition and its nearshore waters.

5. Conclusion:

The present study investigates the migration route of inorganic nutrients to understand the biogeochemical sustainability affected by natural and anthropogenic activities influencing the hyper-turbid Thane creek system (TCS). Results of high-frequency water quality monitoring across the outflow-nearshore gradient and robust statistical analysis results leads to the following conclusions;

- (i) Apparent segmentation found between (i) outflow and nearshore region is related to geographical domination of hydro-physical properties. The nutrients generated by the turbid waters from ephemeral mudflats and periodic dredging are substantially stored in the outflow segment, narrowing its supply to the nearshore due to sluggish water exchange and correspond to year-round bottom TMZ, which influences the creek and nearshore nutrient dynamics.
- (ii) Hypoxic and nutrient rich waters of the upper mesohaline region do not affect outflow and nearshore during post- and pre-monsoon due to meagre exchange. Processes such as disproportional addition and removal of nutrients, mainly nitrogen and phosphorous, occur due to their internal cycling and input from the turbid bottom water. Bottom TMZ corresponds to an increase of PO_4^{3-} in outflow (14 %) and decreased nearshore (35 %), with a net decrease in DSi (5 %) in both segments.

(iii) NH_4^+ sourced from sewage delivered to the outflow region is efficiently mineralized and contributes to nitrogen cycling. The TCS exhibited addition of DIN and PO_4^{3-} by 9 and 14 % in outflow, due to turbid bottom water, which in nearshore are decreased by 10 % (DIN) and 35 % (PO_4^{3-}), indicating significant sinking of transported nitrogen and phosphorous.

(iv) PCA results highlighted the association of nutrients with temperature, with a transitional shift of their stoichiometric ratios indicating temperature as the prime factor for the outflow biological processes. Both nearshore and outflow regions displayed NO_3^- and PO_4^{3-} limiting conditions, among which PO_4^{3-} limitation was predominant conducive to recycling. The inorganic nutrient stoichiometry provided new insight into the chemical water quality index, highlighting un-favourably supportive biological conditions in bottom water.

Acknowledgements

Authors are thankful to Director, CSIR-National Institute of Oceanography (NIO), Goa and Scientist-in-Charge CSIR-NIO, Regional Centre, Mumbai for encouragement towards this study. Analytical measurements done CSIR-NIO; RC Mumbai expenses were met from externally funded Project under OLP 2009. Authors are thankful to all the participants who extended help during fieldwork and analysis. Authors are thankful to the anonymous reviewers for their constructive comments and suggestions on previous version of this article. The article bears CSIR-NIO's contribution No. XXXX.

6. References

- Adame MF, Neil D, Wright SF and Lovelock CE (2010) Sedimentation within and among mangrove forests along a gradient of geomorphological settings. *Estuar Coast Shelf S*, 86(1), pp.21-30. <https://doi.org/10.1016/j.ecss.2009.10.013>.
- Bhavya PS, Kumar S, Gupta GVM, Sudheesh V, Sudharma KV, Varrier DS, Dhanya KR and Saravanane N (2016) Nitrogen uptake dynamics in a tropical eutrophic estuary (Cochin, India) and adjacent coastal waters. *Estuar Coast*, 39(1), pp.54-67. <https://doi.org/10.1007/s12237-015-9982-y>.
- Brown RM, McClelland NI, Deinger RA and O Connor MF (1972) A water quality index-crashing the psychological barrier. In *Indicators of environmental quality*. Springer, Boston, MA. pp. 173-182. https://doi.org/10.1007/978-1-4684-2856-8_15.
- Bruesewitz DA, Gardner WS, Mooney RF and Buskey EJ (2015) Seasonal water column NH₄⁺ cycling along a semi-arid sub-tropical river-estuary continuum: responses to episodic events and drought conditions. *Ecosystems*, 18(5), pp.792-812. <https://doi.org/10.1007/s10021-015-9863-z>.
- Brzezinski MA (1985) The Si: C: N ratio of marine diatoms: Interspecific variability and the effect of some environmental variables 1. *J Phycol*, 21(3), pp.347-357. <https://doi.org/10.1111/j.0022-3646.1985.00347.x>.
- Chouksey MK, Kadam AN and Zingde MD (2004) Petroleum hydrocarbon residues in the marine environment of Bassein–Mumbai. *Mar Pollut Bull*, 49(7-8), pp.637-647. <https://doi.org/10.1016/j.marpolbul.2004.04.007>.
- Cox RA, Culkin F and Riley JP (1967), April. The electrical conductivity/chlorinity relationship in natural sea water. *Deep-Sea Res Els. Vol. 14, No. 2*, pp. 203-220. [https://doi.org/10.1016/0011-7471\(67\)90006-X](https://doi.org/10.1016/0011-7471(67)90006-X).
- Minhan Dai, Lifang Wang, Xianghui Guo, Weidong Zhai, Qing Li, Biyan He, Shuh-Ji Kao.(2008) Nitrification and inorganic nitrogen distribution in a large perturbed river/estuarine system: The Pearl River Estuary, China. *Biogeosciences Discussions*, 5 (2), pp.1545-1585. <https://hal.archives-ouvertes.fr/hal-00297996>.
- Dame R, Bushek DAVID, Allen D, Edwards D, Gregory LEAH, Lewitus A, Crawford SARAH, Koepfler ERIC, Corbett C, Kjerfve B and Prins T (2000) The experimental analysis of tidal creeks dominated by oyster reefs: the pre manipulation year. *J Shellfish Res*, 19(1), pp.361-370.
- de Nijs,MA, Winterwerp JC and Pietrzak JD (2010) The effects of the internal flow structure on SPM entrapment in the Rotterdam Waterway. *J Phys Oceanogr*, 40(11), pp.2357-2380. <https://doi.org/10.1175/2010JPO4233.1>.
- Emmanuel BE. and Onyema IC. (2007) The Plankton and fishes of a tropical creek in South-western Nigeria. *Turk J Fish Aquat Sc*, 7(2), pp.105-113.
- Grasshoff K., Ehrhardt M. and Kremling K (1983) *Methods of Seawater Analysis*, 419 pp., Verlag Chemie.
- Gupta, AK, Gupta SK and Patil RS (2003) A comparison of water quality indices for coastal water. *J Environ Sci Heal A*, 38(11), pp.2711-2725. <https://doi.org/10.1081/ESE-120024458>.

- Gupta I, Dhage S, Chandorkar AA and Srivastav A. (2004) Numerical modeling for Thane creek. *Environ Modell Softw*, 19(6), pp.571-579. <https://doi.org/10.1016/j.envsoft.2003.07.005>.
- Harrison PJ, Thompson PA and Calderwood G.S. (1990) Effects of nutrient and light limitation on the biochemical composition of phytoplankton. *J Appl Phycol*, 2(1), pp.45-56. <https://doi.org/10.1007/BF02179768>.
- Kachroud M, Trolard F, Kefi M, Jebari S and Bourrie G (2019) Water quality indices: Challenges and application limits in the literature. *Water-Sui*, 11(2), p.361. <https://doi.org/10.3390/w11020361>.
- Kessarkar PM, Rao VP, Shynu R, Ahmad IM, Mehra P, Michael GS and Sundar D (2009) Wind-driven estuarine turbidity maxima in Mandovi Estuary, central west coast of India. *J Earth Syst Sci*, 118(4), p.369. <https://doi.org/10.1007/s12040-009-0026-5>.
- Kemp WM, Boynton WR, Adolf JE, Boesch DF, Boicourt WC, Brush G, Cornwell JC, Fisher TR, Glibert PM, Hagy JD and Harding LW (2005) Eutrophication of Chesapeake Bay: historical trends and ecological interactions. *Mar Ecol Prog Ser*, 303, pp.1-29. doi:10.3354/meps303001.
- Kumar, PK, Singh A, Ramesh R and Nallathambi T (2017) N₂ fixation in the Eastern Arabian sea: probable role of heterotrophic diazotrophs. *Front Marine Sc*, 4, p.80. <https://doi.org/10.3389/fmars.2019.00223>.
- Lanoux A, Etcheber H, Schmidt S, Sottolichio A, Chabaud G, Richard M and Abril G (2013) Factors contributing to hypoxia in a highly turbid, macrotidal estuary (the Gironde, France) *Environ Sci-Proc Imp*, 15(3), pp.585-595. <https://doi.org/10.1039/C2EM30874F>.
- Li R, Xu J, Li X, Shi Z and Harrison PJ (2017) Spatiotemporal variability in phosphorus species in the Pearl River estuary: influence of the river discharge. *Sci Rep-Uk*, 7(1), pp.1-13. <https://doi.org/10.1038/s41598-017-13924-w>.
- Liu SM, Li RH, Zhang GL, Wang DR, Du JZ, Herbeck LS, Zhang J and Ren JL (2011) The impact of anthropogenic activities on nutrient dynamics in the tropical Wenchanghe and Wenjiaohe Estuary and Lagoon system in East Hainan, China. *Mar Chem*, 125(1-4), pp.49-68. <https://doi.org/10.1016/j.marchem.2011.02.003>.
- Livingston RJ (1996) Eutrophication in estuaries and coastal systems: relationships of physical alterations, salinity stratification, and hypoxia. *Bel Bar Lib.*, (20), pp.285-318.
- Lohrenz SE, Fahnenstiel GL, Redalje DG, Lang GA, Dagg MJ, Whitley TE and Dortch Q (1999) Nutrients, irradiance, and mixing as factors regulating primary production in coastal waters impacted by the Mississippi River plume. *Cont Shelf Res*, 19(9), pp.1113-1141. [https://doi.org/10.1016/S0278-4343\(99\)00012-6](https://doi.org/10.1016/S0278-4343(99)00012-6).
- Lohrer AM and Wetz JJ (2003) Dredging-induced nutrient release from sediments to the water column in a southeastern saltmarsh tidal creek. *Mar Pollut Bull*, 46(9), pp.1156-1163. [https://doi.org/10.1016/S0025-326X\(03\)00167-X](https://doi.org/10.1016/S0025-326X(03)00167-X).
- Mallin MA and LEWITUS A (2004) Anthropogenic Influences on the Ecology of Tidal Creeks and Canals. *J Exp Mar Biol Ecol*, 298(2). <http://pascal-francis.inist.fr/vibad/index.php?action=getRecordDetail&idt=15407875>.

- Marmontel CVF, Lucas-Borja ME, Rodrigues VA and Zema DA (2018) Effects of land use and sampling distance on water quality in tropical headwater springs (Pimenta creek, São Paulo State, Brazil) *Sci Total Environ*, 622, pp.690-701. <https://doi.org/10.1016/j.scitotenv.2017.12.011>.
- Maya K, Babu KN, Padmalal D and Seralathan P (2007) Hydrochemistry and dissolved nutrient flux of two small catchment rivers, south-western India. *Chem Ecol*, 23(1), pp.13-27. <https://doi.org/10.1080/02757540601084029>.
- Morris AW and Riley JP (1966) The bromide/chlorinity and sulphate/chlorinity ratio in sea water. *Deep-Sea Res Els. Vol. 13, No. 4*, pp. 699-705 [https://doi.org/10.1016/0011-7471\(66\)90601-2](https://doi.org/10.1016/0011-7471(66)90601-2).
- Naidu VS and Sarma RV (2001) Numerical modeling of tide-induced currents in Thane Creek, west coast of India. *J Waterw Port Coast*, 127(4), pp.241-244. [https://doi.org/10.1061/\(ASCE\)0733-950X\(2001\)127:4\(241\)](https://doi.org/10.1061/(ASCE)0733-950X(2001)127:4(241)).
- Swamy GN and Suryanarayana A (1984) Tidal flow characteristics at Kasheli (Kalwa/Bassein Creek), Bombay. *Indian J Mar Sci* 13, 168-171. <http://nopr.niscair.res.in/handle/123456789/38817>.
- Natesan U, Kalaivani S and Kalpana G (2017) Pollution assessment of Ennore (India) creek using macrobenthos. *J. Environ. Geol*, 1, p.10.
- Nayak D and Balaji R (2016) Numerical modeling of tides, currents and waves off Maharashtra coast. *Indian J Mar Sci* 45(10), 1255-1263. <http://nopr.niscair.res.in/handle/123456789/35710>.
- Nixon SW (1995) Coastal marine eutrophication: a definition, social causes, and future concerns. *Ophelia*, 41(1), pp.199-219. <https://doi.org/10.1080/00785236.1995.10422044>.
- Paerl HW (2009) Controlling eutrophication along the freshwater–marine continuum: dual nutrient (N and P) reductions are essential. *Estuaries Coasts*, 32(4), pp.593-601. <https://doi.org/10.1007/s12237-009-9158-8>.
- Painter SC, Hartman SE, Kivimäe C, Salt LA, Clargo NM, Daniels CJ, Bozec Y, Daniels L, Allen S, Hemsley VS and Moschonas G (2017) The elemental stoichiometry (C, Si, N, P) of the Hebrides Shelf and its role in carbon export. *Prog Oceanogr*, 159, pp.154-177. <https://doi.org/10.1016/j.pocean.2017.10.001>.
- Paudel B, Montagna PA and Adams L (2019) The relationship between suspended solids and nutrients with variable hydrologic flow regimes. *Reg Stud in Mar Sci*, 29, p.100657. <https://doi.org/10.1016/j.rsma.2019.100657>.
- Posey MH, Alphin TD and Cahoon L (2006) Benthic community responses to nutrient enrichment and predator exclusion: influence of background nutrient concentrations and interactive effects. *J Exp Mar Biol Ecol*, 330(1), pp.105-118. <https://doi.org/10.1016/j.jembe.2005.12.020>.
- Pradhan UK, Wu Y, Shirodkar PV and Zhang J (2015) Seasonal nutrient chemistry in mountainous river systems of tropical Western Peninsular India. *Chem Ecol*, 31(3), pp.199-216. <https://doi.org/10.1080/02757540.2014.961438>.
- Prati L, Pavanello R and Pesarin F (1971) Assessment of surface water quality by a single index of pollution. *Water res*, 5(9), pp.741-751. [https://doi.org/10.1016/0043-1354\(71\)90097-2](https://doi.org/10.1016/0043-1354(71)90097-2).

- Ptacinik R, Andersen T and Tamminen T (2010) Performance of the Redfield ratio and a family of nutrient limitation indicators as thresholds for phytoplankton N vs. P limitation. *Ecosystems*, 13(8), pp.1201-1214. <https://doi.org/10.1007/s10021-010-9380-z>.
- Quadros G, Mishra V, Ullal V, Gokhale KS and Athalye RP (2001) Status of water quality of Thane creek (India) *Ecol Environ Co* 7, pp.235-240.
- Quadros G, Mishra V, Borkar MU and Athalye RP (2004) Impact of construction and reclamation activities on the water quality of the Thane Creek, Central-west coast of India. *J Coastal Dev*, 7(2), pp.71-78.
- Quadros G, Sukumaran S and Athalye RP (2009) Impact of the changing ecology on intertidal polychaetes in an anthropogenically stressed tropical creek, India. *Aquat Ecol*, 43(4), p.977. <https://doi.org/10.1007/s10452-009-9229-8>.
- Rao VP, Shynu R, Kessarkar PM, Sundar D, Michael GS, Narvekar T, Blossom V and Mehra P (2011) Suspended sediment dynamics on a seasonal scale in the Mandovi and Zuari estuaries, central west coast of India. *Estuarine, Coast Shelf Sci*, 91(1), pp.78-86. <https://doi.org/10.1016/j.ecss.2010.10.007>.
- Reddy BSR and Rao VR (1994) Seasonal variation in temperature and salinity in the Gautami-Godavari estuary. *Proceedings of the Indian Academy Sci-Earth Planet Sci*, 103(1), pp.47-55. <https://doi.org/10.1007/BF02880808>.
- Redfield A, Ketchum B and Richards F (1963) The influence of organisms on the composition of sea-water. In Hill, M. (ed) *The Sea*. Interscience, New York, pp. 26-77.
- Sahu BK, Baliarsingh SK, Srichandan S and Sahu KC (2013) Seasonal variation of zooplankton abundance and composition in Gopalpur creek: a tropical tidal backwater, east coast of India. *J Mar Biol Assoc In*, 55(1), pp.59-64. <https://doi:10.6024/jmbai.2013.55.1.01715-10>.
- Sasamal SK, Rao KH and Suryavansi UM (2007) Sewage and industrial pollution in and around Thane Creek, Mumbai using high resolution IRS data. *Int J Remote Sens*, 28(19), pp.4391-4395. <https://doi.org/10.1080/01431160500354039>.
- Sastry JS (1971) The mechanism of sediment transport in the environs of Bombay harbour. In *Proceedings of the Symposium on the Engineering Properties of Sea-Floor Soils and Their Geophysical Identification*. Washington, UNESCO/University of Washington. (pp. 338-349).
- Schmidt S, Diallo II, Derriennic H, Fallou H and Lepage M (2019) Exploring the susceptibility of turbid estuaries to hypoxia as a prerequisite to designing a pertinent monitoring strategy of dissolved oxygen. *Frontiers Mar Sci*, 6, p.352. <https://doi.org/10.3389/fmars.2019.00352>.
- Shirodkar PV, Mesquita A, Pradhan UK, Verlekar XN, Babu MT and Vethamony P (2009) Factors controlling physico-chemical characteristics in the coastal waters off Mangalore-a multivariate approach. *Environmental Res*, 109(3), pp.245-257. <https://doi.org/10.1016/j.envres.2008.11.011>.
- Singare PU, Lokhande RS and Pathak PP (2010) Study on physico-chemical properties and heavy metal content of the soil samples from Thane Creek of Maharashtra, India. *Interdi Environm Rev*, 11(1), pp.38-56. <https://doi.org/10.1504/IER.2010.034605>.

- Sylvan JB, Quigg A, Tozzi S and Ammerman JW, (2007) Eutrophication- induced phosphorus limitation in the Mississippi River plume: Evidence from fast repetition rate fluorometry. *Limnol Oceanogr*, 52(6), pp.2679-2685. <https://doi.org/10.4319/lo.2007.52.6.2679>.
- Thanh-Nho N, Marchand C, Strady E, Van Vinh T, Taillardat P, Cong-Hau N and Nhu-Trang TT (2020) Trace metal dynamics in a tropical mangrove tidal creek: influence of porewater seepage (Can Gio, Vietnam) *Frontier Environ Sci*. DOI : 10.3389/fenvs.2020.00139.
- Thomas J, Velamala SN and Prasad KVSR (2019) Numerical Simulation of Tidal Constituents in Thane Creek and the Ulhas Estuary, West Coast of India. *J Coastal Res*, 35(2), pp.376-388. <https://doi.org/10.2112/JCOASTRES-D-17-00189.1>.
- Thrane JE, Hessen DO and Andersen T (2017) Plasticity in algal stoichiometry: Experimental evidence of a temperature- induced shift in optimal supply N: P ratio. *Limnol Oceanogr*, 62(4), pp.1346-1354. <https://doi.org/10.1002/lno.10500>.
- Vijay R, Khobragade PJ, Sohony RA, Kumar R and Wate SR (2014) Hydrodynamic and water quality simulation of Thane creek, Mumbai: an impact of sewage discharges. *Indian J Mar Sci* 43(10), 519-526. <http://hdl.handle.net/123456789/34541>.
- Vijay R, Dey J, Sakhre S and Kumar R (2020) Impact of urbanization on creeks of Mumbai, India: a geospatial assessment approach. *J Coast Conserv*, 24(1), pp.1-16. <https://doi.org/10.1007/s11852-019-00721-y>.
- Winterwerp JC, Vroom J, Wang ZB, Krebs M, Hendriks EC, van Maren DS, Schrottke K, Borgsmüller C and Schöl A (2017) SPM response to tide and river flow in the hyper-turbid Ems River. *Ocean Dynam*, 67(5), pp.559-583. <https://doi.org/10.1007/s10236-017-1043-6>.
- Zingde, M.D. and Govindan, K., (2000) Health status of the coastal waters of Mumbai and regions around.

Figure 1: Upper: map of Thane creek system (TCS) along the western peninsular India with its confluence in the freshwater region of Ulhas river. The mesohaline regime is marked in grey (Quadros et al., 2001). Freshwater discharge (red star) and rainfall stations (blue circle; Indian Meteorological Department) are marked on the map. Lower: map showing creek outflow and nearshore areas of TCS, with sampling locations for water quality measurement. The current direction during ebb-tide is marked with solid arrow and tide-induced residual circulation is marked with dotted grey arrow adopted from Naidu and Sarma, 2001.

Figure 2: (a) Mean monthly rainfall proportions to the annual rainfall during 2017-18, with deviation from long-term (1982-2012; IMD) indicating disproportionate rainfall between upper and lower Thane creek system (TCS) influenced with sporadic extreme events. (b) Fluvial load at Badlapur, Ulhas river, the prime source of freshwater and suspended sediment to TCS indicated sporadic flood events during late southwest monsoon (Data: Central Water Commission, India).

Figure 3: Results of hierarchical cluster analysis presented through dendrogram. Stations around the Thane creek outflow and nearshore region are grouped based on their similar hydrography characteristics during different seasons.

Figure 4: Monthly (mean $\pm 2\sigma$ standard error) data on hydrographic properties within surface (n=382) and bottom (n=382) layers of outflow as well as nearshore segments during 2017-18. Variation in air temperature, turbidity and DO_{sat} are presented along with water temperature, SPM and DO, respectively to highlight the close resemblance among them.

Figure 5: Monthly (mean $\pm 2\sigma$ standard error) nutrient composition within surface (n=382) and bottom (n=382) layers of outflow as well as nearshore segments during 2017-18.

Figure 6: Nutrient stoichiometric plots for a) outflow and b) nearshore revealing seasonal shift in inorganic nutrient pool in Thane creek system. The vertical pink lines, horizontal blue lines and diagonal black lines represent stoichiometric ratios based on the standard stoichiometric formula (15Si:16N:1P; Redfield et al., 1963).

Figure 7: (a-b) PCA analysis of seasonal data indicating two prime factors responsible of nutrient composition change with respect to hydrography in nearshore and outflow segment. (c-d) monthly (mean $\pm 2\sigma$ standard error) data on chemical water quality index (CWQI) within surface (n=382) and bottom (n=382) layers of outflow as well as nearshore segments during 2017-18 indicating overall good water quality (CWQI= >60-90) in outflow and nearshore. Sporadic un-supportive conditions noticed in bottom water as indicated through classes I: Supportive; II: fairly supportive; III: un-supportive are based on the nutrient stoichiometric response to the biological functioning indicated as solid lines (surface: orange and Bottom: blue).

Table 1: Mean ($\pm 2\sigma$) values of hydrographic parameters across outflow-nearshore segment, with their statistical differences during different seasons as well as between surface and bottom layers presented to significance level ($p < .05$, $p < .01$); ns=not significant.

Table 2: Mean ($\pm 2\sigma$) values of nutrients and stoichiometric ratios across outflow-nearshore segment, with their statistical differences during different seasons as well as between surface and bottom layers presented to significance level ($p < .05$, $p < .01$); ns=not significant.

Table 3: Inter-relationship among the hydrography and nutrient parameters across outflow-nearshore segment, during different seasons marked through Pearson's correlation analysis (r) and presented to significance level (** $p < .01$, * $p < .05$); ns=not significant.

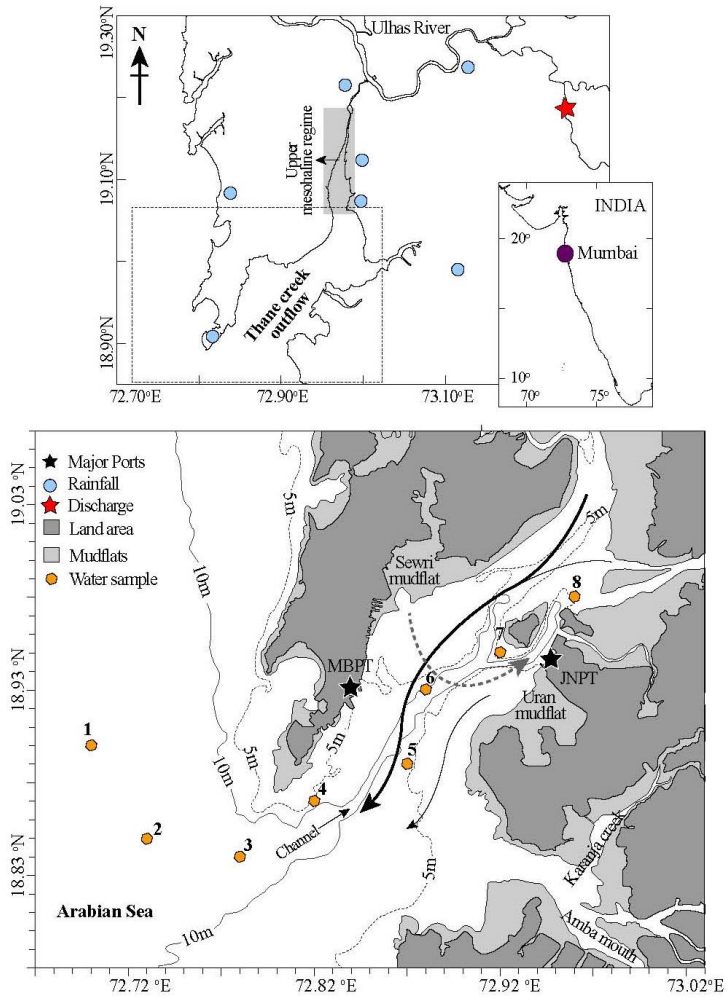


Figure 1:

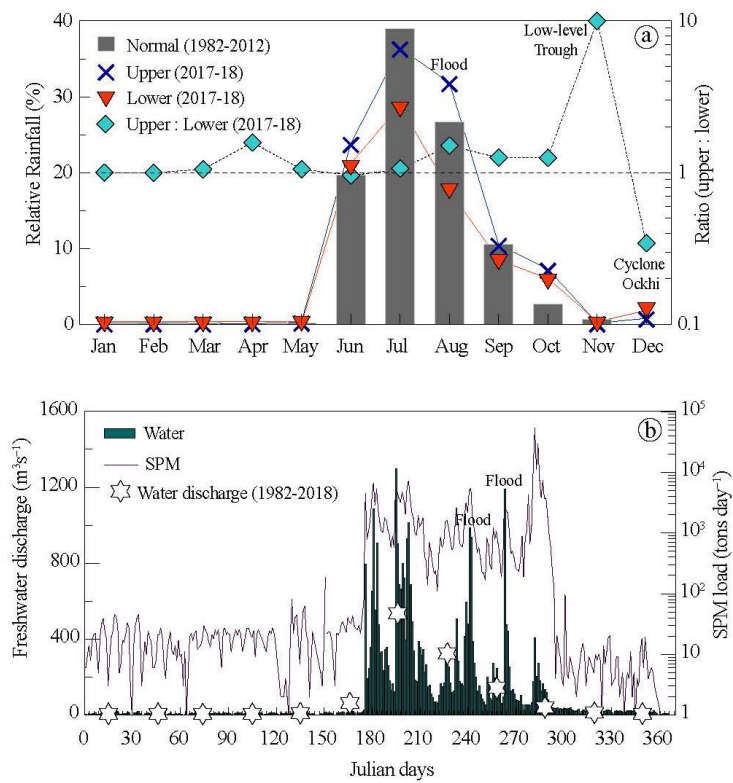


Figure 2:

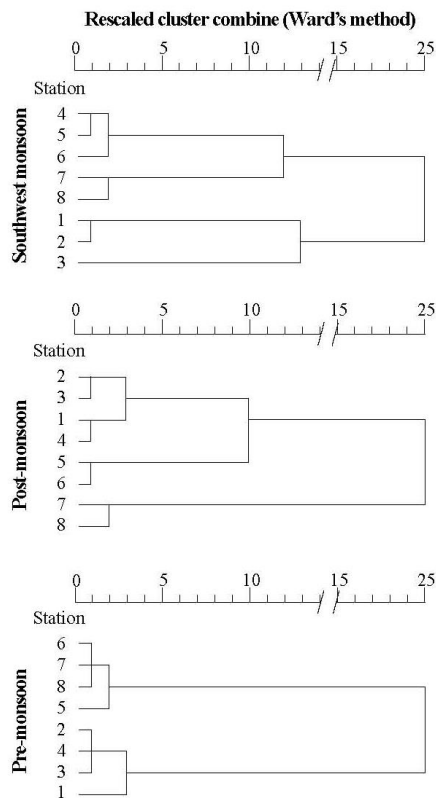


Figure 3:

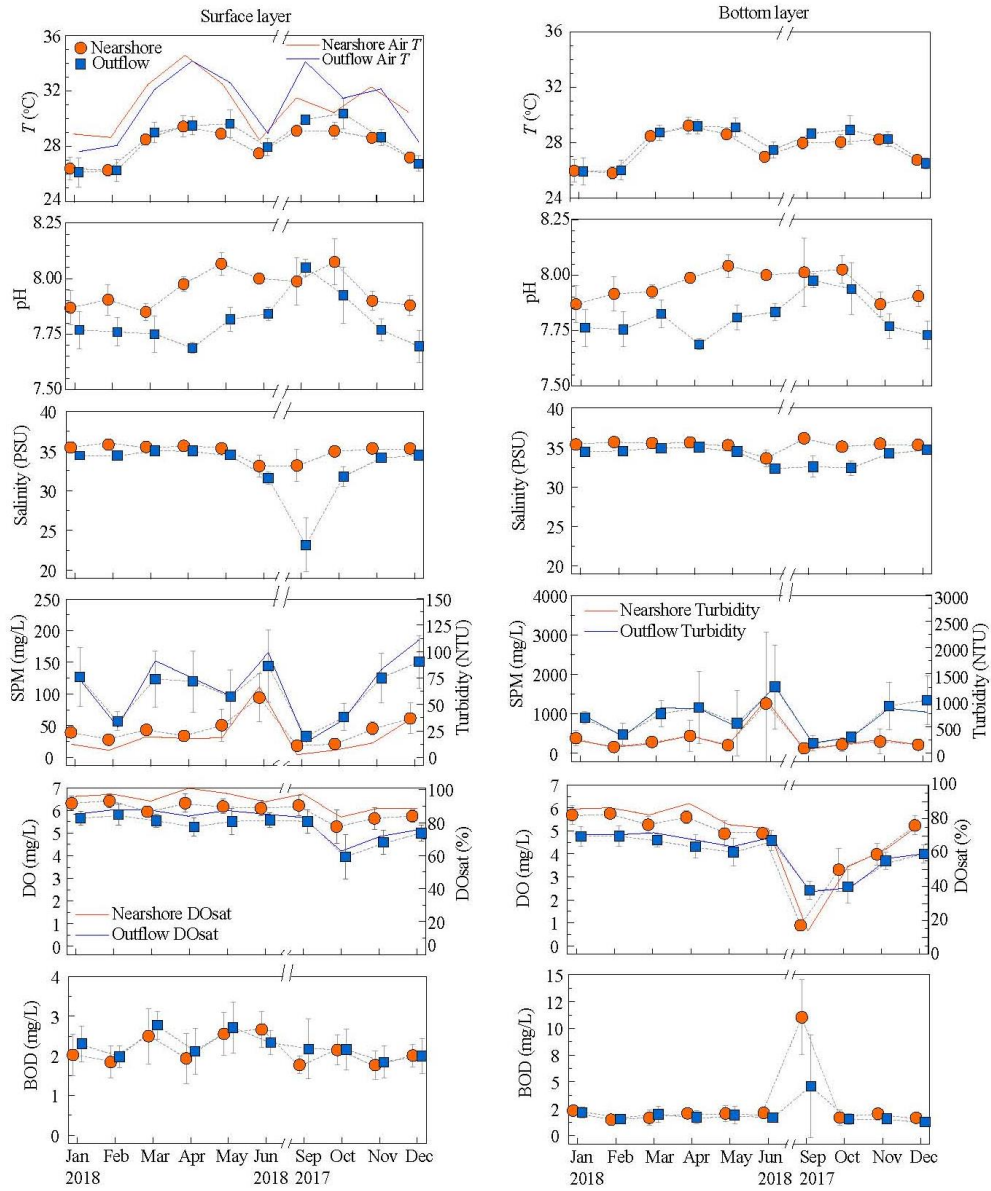


Figure 4:

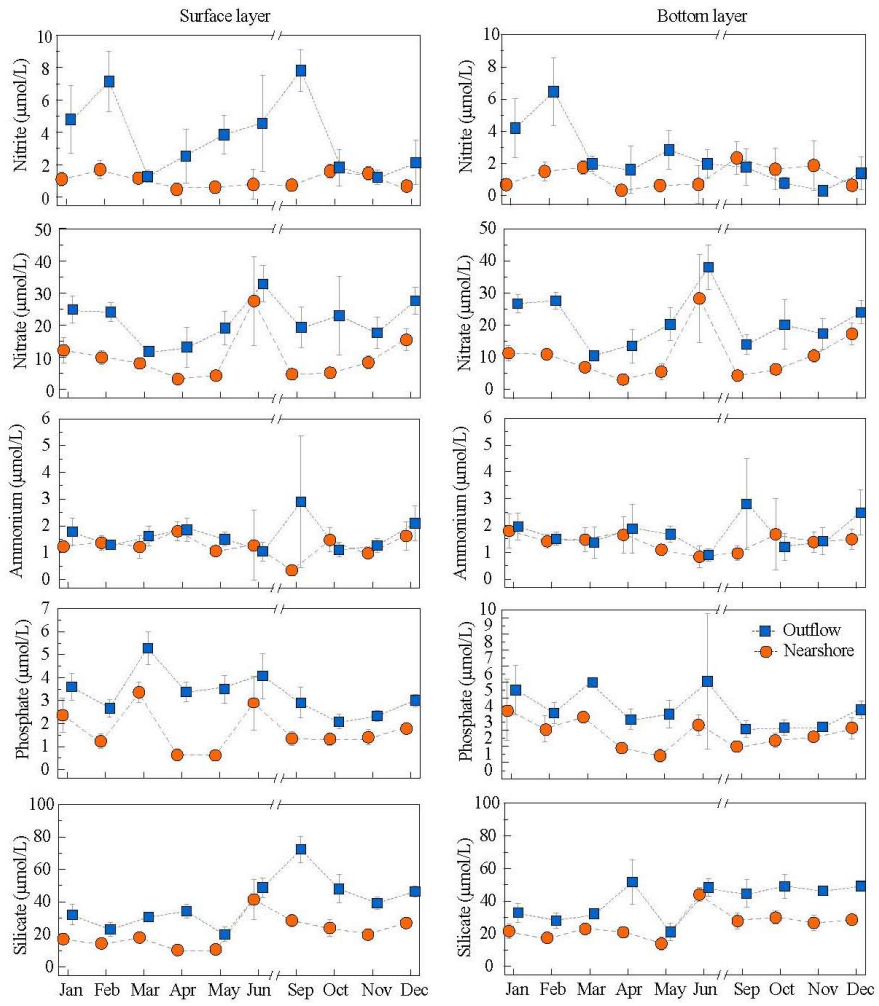


Figure 5:

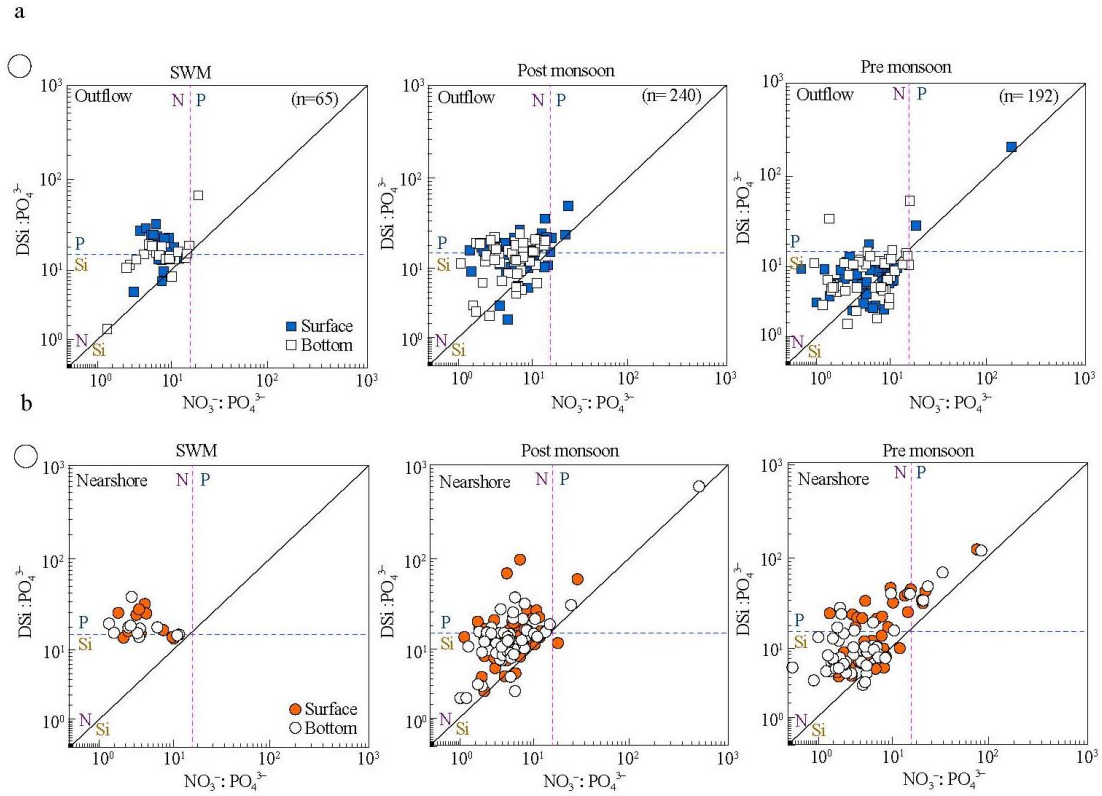


Figure 6:

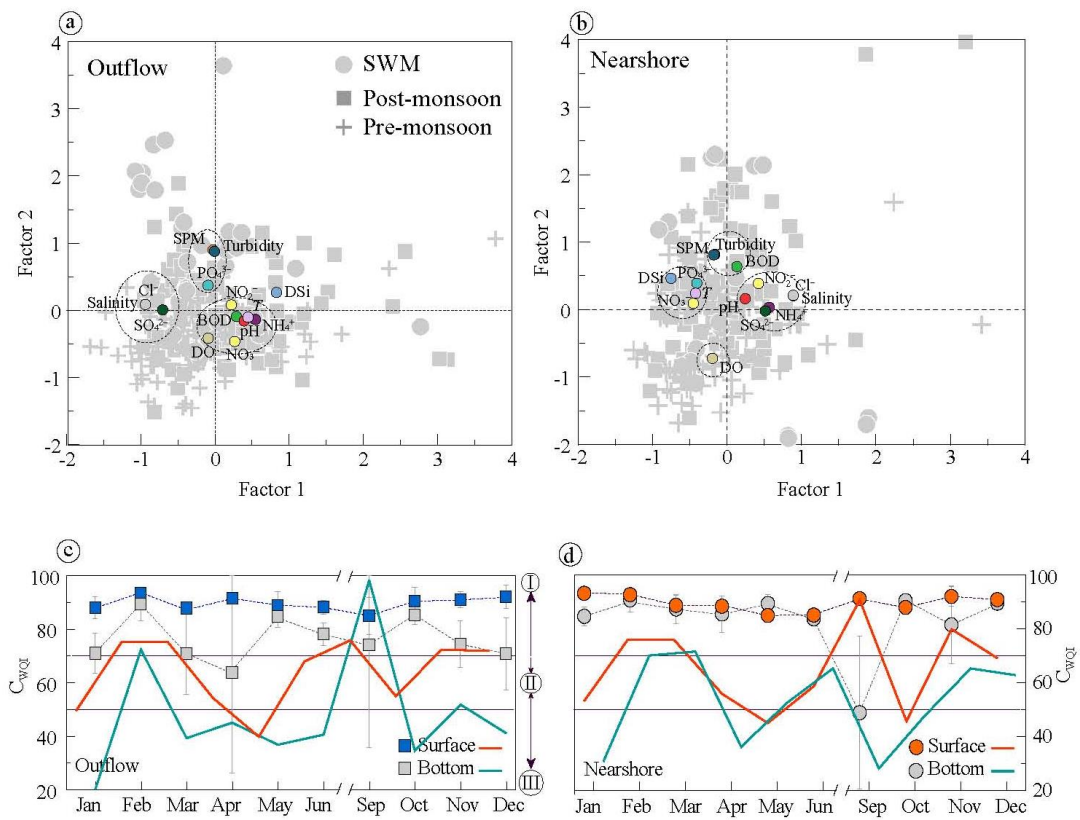


Figure 7:

Table 1: Mean ($\pm 2\sigma$) values of hydrographic parameters across outflow-nearshore segment, with their statistical differences during different seasons as well as between surface and bottom layers presented to significance level ($p < .05$, $p < .01$); ns=not significant.

Layer	Season	Region	Salinity PSU	T °C	pH	DO mgL ⁻¹	BOD mgL ⁻¹	SPM mgL ⁻¹	Turbidity NTU
Surface	SWM	Nearshore	33.1±2.5	28.7±0.8	8±0.1	6.2±0.6	2±0.5	39.1±39.6	21±33.6
		Outflow	28.2±5.3	28.8±1.3	7.9±0.1	5.6±0.6	2.3±0.8	99.9±94.8	65.5±69.5
		All	30 ± 5.1	28.7 ± 1.1	7.9 ± 0.1	5.8 ± 0.7	2.2 ± 0.7	78.3 ± 84.2	49.7 ± 62.5
	Post-monsoon	Nearshore	35.3±0.6	27.6±1.5	7.9±0.1	5.8±0.9	2±0.8	46.1±36.1	20.2±32.2
		Outflow	34±1.4	27.6±2.1	7.8±0.2	4.9±1.1	2.1±0.9	126±87.3	83.8±67.6
		All	34 ± 1.4	28.4 ± 1.4	7.9 ± 0.2	5.3 ± 1.2	2.1 ± 0.8	58 ± 57.5	29.9 ± 46.5
	Pre-monsoon	Nearshore	35.6±0.4	27.8±1.6	7.9±0.1	6.3±0.6	2.1±1	37.1±25.4	13.7±21.3
		Outflow	34.6±0.8	28.1±2.2	7.8±0.1	5.6±0.9	2.3±0.9	88.3±62.8	54.7±53.8
		All	35 ± 0.9	27.9 ± 1.6	7.8 ± 0.1	5.7 ± 0.7	2.2 ± 0.9	64.6 ± 53.9	39.3 ± 48.6
<i>p-value</i>	<i>SWM</i>	<i>Nearshore vs. outflow</i>	≤ .01	ns	ns	≤ .01	ns	< .05	ns
	<i>Post-monsoon</i>	<i>Nearshore vs. outflow</i>	< .01	ns	< .01	< .01	ns	< .01	< .01
	<i>Pre-monsoon</i>	<i>Nearshore vs. outflow</i>	< .01	ns	< .01	< .01	ns	< .01	< .01
		<i>Seasonal (All)</i>	< .01	≤ .01	< .01	< .01	ns	< .05	ns
Bottom	SWM	Nearshore	35.5±1.3	27.7±0.7	8±0.2	2±1.9	8.6±5.9	433.9±894.8	335.2±741
		Outflow	32.4±1.5	28±1	7.9±0.1	3.7±1.3	2.8±4.5	1112.5±1606.6	828.6±1170.1
		All	33.5 ± 2	27.9 ± 0.9	7.9 ± 0.1	3.1 ± 1.7	4.9 ± 5.7	871.7 ± 1418	653.6 ± 1052.5
	Post-monsoon	Nearshore	35.4±0.6	27.1±1.4	7.9±0.1	4.8±1.3	1.9±1	280.8±402.7	207.8±321
		Outflow	34.2±1.2	27.2±1.8	7.8±0.2	3.9±1.1	1.6±0.9	1064.2±1068.8	711.6±591
		All	34.3 ± 1.2	27.8 ± 1.1	7.9 ± 0.2	3.9 ± 1.3	1.6 ± 0.8	836 ± 1294	502.6 ± 731.8
	Pre-monsoon	Nearshore	35.6±0.4	27.5±1.7	7.9±0.1	5.4±0.7	1.7±1	237.2±282.3	162±238.5
		Outflow	34.7±0.8	27.8±2	7.8±0.1	4.5±0.9	1.7±1	749.1±1018.4	548.6±691.8
		All	35 ± 0.8	27.7 ± 1.6	7.8 ± 0.2	4.9 ± 0.8	1.9 ± 0.8	573.5 ± 601	428.7 ± 480.4
<i>p-value</i>	<i>SWM</i>	<i>Nearshore vs. outflow</i>	< .01	ns	< .05	< .01	< .01	ns	ns
	<i>Post-monsoon</i>	<i>Nearshore vs. outflow</i>	< .01	ns	< .01	< .01	ns	< .01	< .01
	<i>Pre-monsoon</i>	<i>Nearshore vs. outflow</i>	< .01	ns	< .01	< .01	ns	< .01	< .01
		<i>Seasonal (All)</i>	< .01	< .05	< .05	< .01	< .01	ns	ns
<i>p-value</i>	<i>SWM</i>	<i>Surface vs. Bottom</i>	< .01	< .01	ns	< .01	< .05	< .01	< .01
	<i>Post-monsoon</i>	<i>Surface vs. Bottom</i>	ns	< .05	ns	< .01	< .05	< .01	< .01
	<i>Pre-monsoon</i>	<i>Surface vs. Bottom</i>	ns	ns	ns	< .01	< .01	< .01	< .01

Standard: Hydrography [*T*:26.3 °C; *pH*:6.5-8.5; *DO*:3 mg/L; *BOD*:3 mg/L; *SPM*:42.9 mg/L; *Turbidity*: 30 NTU]; Nutrient (μmol/L) [*PO₄³⁻*: 0.5-1.4; *NO₃⁻*: 2; *NH₄⁺*:1]
 Permissible: Hydrography [*T*:34 °C; *pH*:6.5-9.0; *DO*:4-5 mg/L; *BOD*:5 mg/L; *SPM*:100 mg/L; *Turbidity*: 100 NTU; *SO₄²⁻*:2.71 g/kg; *Cl*:19.37 g/kg] Nutrient (μmol/L)
 [*PO₄³⁻*: 161; *NO₃⁻*: 1429; *NH₄⁺*:357] (Morries and Riley, 1966; Central Pollution Control Board, 1986, 2000; CSIR NIO Technical Report, 2019; Gupta et al., 2003; NCCR, 2018; Shankarnarayanan and Reddy,1986; Sargaonkar and Deshpande, 2003)

Table 2: Mean ($\pm 2\sigma$) values of nutrients and stoichiometric ratios across outflow-nearshore segment, with their statistical differences during different seasons as well as between surface and bottom layers presented to significance level ($p < .05$, $p < .01$); ns=not significant.

Layer	Season	Region	SO ₄ ²⁻ g/kg	PO ₄ ³⁻ μmol/L	NO ₃ ⁻ μmol L ⁻¹	NH ₄ ⁺ μmol/L	NO ₂ ⁻ μmol/L	DSi μmol/L	NO ₃ ⁻ : PO ₄ ³⁻	DSi: PO ₄ ³⁻	NO ₃ ⁻ :DSi
Surface	SWM	Nearshore	2.4±0.2	1.8±0.9	11±12	0.6±0.7	0.7±0.4	32±9	5.1 ± 2.8	20.6 ± 6.9	0.3 ± 0.2
		Outflow	2.1±0.4	3.6±1.6	27.4±11.6	1.8±2.4	5.9±4.5	58.2±16	7.7 ± 2.2	18.3 ± 7.5	0.5 ± 0.3
		All	2.2 ± 0.4	3 ± 1.6	21.6 ± 14.1	1.4 ± 2	4 ± 4.3	48.9 ± 18.7	6.8 ± 2.7	19.1 ± 7.3	0.4 ± 0.3
	Post-monsoon	Nearshore	2.5±0.3	1.8±1	11.3±7.4	1.3±0.8	1.1±0.8	22±7.6	6.8 ± 4.3	16.6 ± 14.8	0.5 ± 0.3
		Outflow	2.2±0.5	2.9±0.9	23.6±11.1	1.7±1.1	2.5±3.2	40.8±11.6	8.7 ± 4.5	15.9 ± 7.5	0.6 ± 0.4
		All	2.6 ± 0.2	1.9 ± 0.8	13.3 ± 12.3	1.6 ± 1.3	1.2 ± 1	32.1 ± 13.4	7.8 ± 4.5	16.3 ± 11.7	0.6 ± 0.4
	Pre-monsoon	Nearshore	2.5±0.3	1.3±1.1	7.1±4.5	1.3±0.6	1.1±1	13.4±5.7	8.6 ± 11.3	18.1 ± 19.2	0.5 ± 0.3
		Outflow	2.7±0.1	3.4±1.3	19±8.6	1.5±0.5	4.6±3.9	25.4±9.3	9.7 ± 25.4	12 ± 29.2	0.9 ± 0.6
		All	2.5 ± 0.2	2.8 ± 1.7	14 ± 8.8	1.3 ± 0.6	2.5 ± 3.2	22.9 ± 9.6	9.1 ± 19.6	15.1 ± 24.8	0.7 ± 0.5
<i>p-value</i>	<i>SWM</i>	<i>Nearshore vs. outflow</i>	ns	< .01	< .01	ns	< .01	< .01	< .01	ns	< .05
	<i>Post-monsoon</i>	<i>Nearshore vs. outflow</i>	0.01	< .01	< .01	ns	< .01	< .01	< .05	ns	ns
	<i>Pre-monsoon</i>	<i>Nearshore vs. outflow</i>	< .05	< .01	< .01	ns	< .01	< .01	ns	ns	< .01
		<i>Seasonal (All)</i>	< .01	ns	≤ .01	ns	< .01	< .01	ns	ns	< .01
Bottom	SWM	Nearshore	2.7±0.1	1.9±0.8	10.9±12.5	0.9±0.4	1.9±1.5	32.2±9.7	4.9 ± 3.4	18.7 ± 7	0.3 ± 0.3
		Outflow	2.5±0.2	4.4±5.9	28.4±15.5	1.7±1.8	1.9±1.5	46.9±10.5	8.7 ± 4.7	16.7 ± 12.5	0.6 ± 0.3
		All	2.6 ± 0.2	3.5 ± 4.8	22.2 ± 16.6	1.4 ± 1.5	1.9 ± 1.5	41.7 ± 12.4	7.3 ± 4.6	17.4 ± 10.8	0.5 ± 0.3
	Post-monsoon	Nearshore	2.7±0.1	2.7±2.3	12.4±6.7	1.6±1.1	1.1±1.9	26.4±8.3	13.9 ± 64.7	22.5 ± 74.5	0.5 ± 0.3
		Outflow	2.5±0.1	3.7±2	22.4±9.1	1.9±1.4	1.8±2.8	44±10.8	6.8 ± 3.2	14 ± 5.5	0.6 ± 0.3
		All	2.6 ± 0.1	2.7 ± 1.3	13.2 ± 8.8	1.8 ± 1.7	1.1 ± 2	36.4 ± 12.3	10.4 ± 45.7	18.3 ± 52.8	0.5 ± 0.3
	Pre-monsoon	Nearshore	2.5±0.3	2.1±1.5	7.6±4.2	1.4±0.6	1.1±1.1	18.1±7.4	7.1 ± 13.2	15.1 ± 19.6	0.5 ± 0.3
		Outflow	2.6±0.2	3.8±1.5	20.6±9.4	1.6±0.8	4±4	30.9±15.1	6.5 ± 4.3	9.7 ± 8.6	0.9 ± 0.7
		All	2.4 ± 0.2	3.5 ± 1.8	13.7 ± 9	1.3 ± 0.7	2.5 ± 3.6	29.5 ± 11.4	6.8 ± 9.7	12.4 ± 15.3	0.7 ± 0.6
<i>p-value</i>	<i>SWM</i>	<i>Nearshore vs. outflow</i>	< .01	ns	< .01	ns	ns	< .01	< .05	ns	< .05
	<i>Post-monsoon</i>	<i>Nearshore vs. outflow</i>	< .01	< .01	< .01	ns	ns	< .01	ns	ns	ns
	<i>Pre-monsoon</i>	<i>Nearshore vs. outflow</i>	ns	< .01	< .01	ns	< .01	< .01	ns	ns	< .01
		<i>Seasonal (All)</i>	ns	ns	< .01	ns	< .01	< .01	ns	ns	< .05
<i>p-value</i>	<i>SWM</i>	<i>Surface vs. Bottom</i>	< .01	ns	ns	ns	< .05	ns	ns	ns	ns
	<i>Post-monsoon</i>	<i>Surface vs. Bottom</i>	< .01	< .01	ns	ns	ns	< .05	ns	ns	ns
	<i>Pre-monsoon</i>	<i>Surface vs. Bottom</i>	ns	< .05	ns	ns	ns	< .01	ns	ns	ns

Table 3: Inter-relationship among the hydrography and nutrient parameters across outflow-nearshore segment, during different seasons marked through Pearson's correlation analysis (r) and presented to significance level (** $p < .01$, * $p < .05$); ns=not significant.

Season	Parameters	Nearshore		Outflow	
		Salinity	SPM	Salinity	SPM
SWM	DO	-.709**	ns	-.381*	ns
	BOD	.522*	ns	ns	ns
	SO ₄ ²⁻	.706**	ns	.957**	ns
	PO ₄ ³⁻	ns	ns	ns	ns
	NO ₃ ⁻	ns	ns	ns	ns
	NH ₄ ⁺	ns	ns	-.563**	ns
	NO ₂ ⁻	.555**	ns	-.520**	ns
	DSi	-.445*	ns	-.862**	ns
Post monsoon	DO	ns	-.285**	.224*	-.194*
	BOD	ns	ns	ns	ns
	SO ₄ ²⁻	ns	ns	ns	ns
	PO ₄ ³⁻	-.228*	.452**	ns	.229*
	NO ₃ ⁻	ns	ns	ns	ns
	NH ₄ ⁺	ns	ns	ns	ns
	NO ₂ ⁻	ns	.641**	-.342**	ns
	DSi	ns	.279**	-.309**	ns
Pre monsoon	DO	.446**	-.280**	.358**	-.224*
	BOD	-.308**	ns	ns	ns
	SO ₄ ²⁻	.784**	-.521**	.561**	-.543**
	PO ₄ ³⁻	ns	.239*	ns	.235*
	NO ₃ ⁻	ns	ns	-.284**	ns
	NH ₄ ⁺	.289**	.234*	ns	ns
	NO ₂ ⁻	ns	ns	-.309**	-.215*
	DSi	-.281**	.466**	ns	.537**